remote sensing

MDPI

Article

Accelerated Glacier Area Loss in the Zhetysu (Dzhungar) Alatau Range (Tien Shan) for the Period of 1956–2016

Serik Nurakynov [1,2], Azamat Kaldybayev [1,3,4,*], Kanat Zulpykharov [1,3], Nurmakhambet Sydyk [1,3], Aibek Merekeyev [1], Daniker Chepashev [1], Aiman Nyssanbayeva [3], Gulnura Issanova [5] and Gonghuan Fang [4]

1 Institute of Ionosphere, Almaty 050000, Kazakhstan
2 Department of Surveying and Geodesy, Satbayev University, Almaty 050000, Kazakhstan
3 Faculty of Geography and Environmental Sciences, Al-Farabi Kazakh National University, Almaty 050000, Kazakhstan
4 State Key Laboratory of Desert and Oasis Ecology, Xinjiang Institute of Ecology and Geography, Chinese Academy of Sciences, Urumqi 830011, China
5 Research Centre for Ecology and Environment of Central Asia, Almaty 050060, Kazakhstan
* Correspondence: azamat.kaldybayev@gmail.com

Abstract: An updated glacier inventory is important for understanding the current glacier dynamics in the conditions of actual accelerating glacier retreat observed around the world. Here, we present a detailed analysis of the glaciation areas of the Zhetysu Alatau Range (Tien Shan) for 1956–2016 using well-established semiautomatic methods based on the band ratios. The total glacier area decreased by 49 ± 2.8% or by 399 ± 11.2 km^2 from 813.6 ± 22.8 km^2 to 414.6 ± 11.6 km^2 during 1956–2016, while the number of glaciers increased from 985 to 813. Similar rates of area change characterized the periods 1956–2001, 2001–2012, 2012–2016, and 2001–2016: −296.2 ± 8.3 (−0.8% a^{-1}), −63.7± 1.8 (−1.1% a^{-1}), −39.1 ±1.1 (−2.2% a^{-1}) and −102.8 ± 2.9 (−1.3% a^{-1}) km^2, respectively. The mean glacier size decreased from 0.57 km^2 in 2001 to 0.51 km^2 in 2016. Most glaciation areas of the Zhetysu Alatau faced north (north, northwest, and northeast), covered 390.35 ± 11 km^2, and were located in altitudes between 3000 and 4000 m.a.s.l. With shrinkage rates of about −0.8% and −1.3% a^{-1} for the periods of 1956–2001 and 2001–2016, our results show that study area has the highest shrinkage rate compared to other glacierized areas of Central Asian mountains, including Altai, Pamir, and even the inner ranges of Tien Shan. It was found that a significant increase in temperature (0.12 °C/10 years) plays a main role in the state of glaciers.

Keywords: inventory; glacier shrinkage; climate change; Eastern Tien Shan; the Zhetysu (Dzhungar) Alatau

Citation: Nurakynov, S.; Kaldybayev, A.; Zulpykharov, K.; Sydyk, N.; Merekeyev, A.; Chepashev, D.; Nyssanbayeva, A.; Issanova, G.; Fang, G. Accelerated Glacier Area Loss in the Zhetysu (Dzhungar) Alatau Range (Tien Shan) for the Period of 1956–2016. *Remote Sens.* **2023**, *15*, 2133. https://doi.org/10.3390/rs15082133

Academic Editors: Ulrich Kamp, Shridhar Jawak and Dariusz Ignatiuk

Received: 2 March 2023
Revised: 5 April 2023
Accepted: 14 April 2023
Published: 18 April 2023

1. Introduction

In arid and semiarid regions with a low amount of precipitation during the summer, glaciers play a vital role in forming river flow, as melt water is released from the ice when other sources, such as melting snow and the end of the wet season, are exhausted [1,2]. The function of glaciers as a "Water Tower" is of great importance, especially in arid regions, where there is often a shortage of water in the form of rain and snow [3,4]. This case is clearly visible in the Tien Shan, one of the largest mountain systems in the world, located in the Central Asian region. Here, in the summer, glaciers make a significant contribution to the provision of fresh water reserves in the densely populated arid lowlands of Kyrgyzstan, Kazakhstan, Uzbekistan, Turkmenistan, and Xinjiang (China) [5–7].

The semiarid and arid climate typical of most regions of Central Asia is characterized by unique water-dependent ecosystems, and for millennia, human communities have developed in close interaction with limited natural water resources such as rivers, lakes, and areas of shallow groundwater [8]. It has been demonstrated that even a basin with a <5% glacier surface fraction can provide significant amounts of meltwater, contributing to

river runoff during summer, when water is needed most for irrigation [7,9]. People living in the dry lowlands of Central Asia (irrigated agricultural land and oases) depend on river waters originating from the Tien Shan mountains [10].

Arid lowlands and deserts, where irrigation during the growing season usually depends on glacial meltwater, are common along the entire border of the Zhetysu Alatau (Dzhungar) mountain range. In our study area, the waters of the Karatal, Koksu, Lepsy, Aksu, and other rivers are intensively used for irrigation. In the basins of these rivers, the water withdrawal for irrigation of almost 200 thousand hectares is estimated at 1.3 km^3/year. Rational water use for irrigation and hydropower needs is impossible without comprehensive information on the glaciation areas change (shrinkage) and their volume. Glacier shrinkage leads to a reduction in their long-term moisture reserve, glacial runoff decrease, and the violation of the natural self-regulation of river flow. This problem is solved by monitoring modern glaciation, which should be carried out not for 1–2 "reference" glaciers of a mountainous country where field observations are carried out (an example is the well-known Tuyuksu glacier in the Ile Alatau), but for large glacial systems in general, numbering hundreds and thousands of glaciers. It is also necessary to assess the rate of reduction in ice reserves and the prospects for the existence of these systems in the near and distant future [11].

The first detailed inventory of the Zhetysu Alatau glaciers, the Catalog of Glaciers (*Catalogue of Glaciers of the USSR*, 1969, 1970, 1975, and 1980), was published in 1969 and was based on aerial photographs from 1956. Cherkasov (2004) compiled a second glacier inventory using 1:25,000 topographic maps based on aerial photographs taken in 1972. However, two more limited surveys of glaciers conducted in the 1990s and 2000s have not been released [12].

In subsequent years, several authors studied the glacier area change in the entire Zhetysu Alatau and its subregions. They estimated the overall glacier area decrease [13–15]. The study by Severskiy et al. [15] was especially detailed, where the authors conducted a general analysis and assessment of changes in the glaciation areas of the entire Zhetysu Alatau (in 1956, 1972, 1990, 2000, and 2011). They analyzed changes between 1956 and 1972 based on the glacier catalog of the USSR, which was created using topographic maps at a scale of 1:25,000 based on aerial photographs taken in 1972. Our catalog of the Zhetysu Alatau glaciers was carried out for 2000 and 2011, similar to the catalog content mentioned above, on the basis of state survey maps at a scale of 1:25,000, Landsat 7 ETM+ satellite images, a digital elevation model (DEM), and surface reference points. According to their studies, Severskiy et al. [15], in the period 1956–2011, found that the area of glaciers of the Zhetysu Alatau decreased from 813.9 km^2 [16–19] to 465.17 km^2, and the total annual reduction rate was 0.78%. Owing to climate change and other factors, over the past few decades, nearly 97.52% of glaciers in the Tien Shan mountains have been shrinking at a rapid rate [20], characterized by a decrease in the total area and mass of glaciers by about $27 \pm 15\%$ [4], as well as the fact that, in the near future, this process of shrinking glaciers will continue [21,22].

Despite the vulnerability of the Zhetysu Alatau glaciers to area shrinkage in the region [13], ground monitoring and actual area assessment have not been carried out during recent years since 2012. Thus, a continuous glacier inventory is essential in the Zhetysu Alatau.

The main aim of this article is the investigation of glaciers and their changes in the Kazakh part of the Zhetysu Alatau based on remote sensing data. In particular, the major objectives are: (1) to create an updated catalog of the Zhetysu Alatau glaciers using remotely sensed data, to obtain and analyze the characteristics of glaciers in order to compare them with other previous inventory works, (2) to analyze the glacier area change dynamics from 1956 to 2016, (3) to analyze the main climatic trends (temperature and precipitation), (4) and to correlate the estimated changes in glacier areas with climatic, topographic parameters, and other characteristics.

2. Study Area

The Zhetysu Alatau (Dzhungar Alatau) is a mountain system stretching from west–southwest to east–northeast along the state border between Kazakhstan and China. The range length is 450 km, the width fluctuates from 50 to 90 km, and the maximal height reaches up to 4622 m (Semyonov-Tyan-Shansky peak) (Figure 1). The total area of the Zhetysu Alatau mountain ridge, including the river basins of the Borotala Mountains in China, is about 40,000 km^2 [23]. It is located at 45° N, within 79–82°E. Its southern border is the Ile River, the northern one is the Balkhash Plain, and the northeastern one is the Alakol Lake and Dzhungar Gates. The longitudinal valleys of the rivers Koksu in the west and Borotala in the east divide the Zhetysu Alatau into two large ridges parallel to each other—North Central and South Central [24].

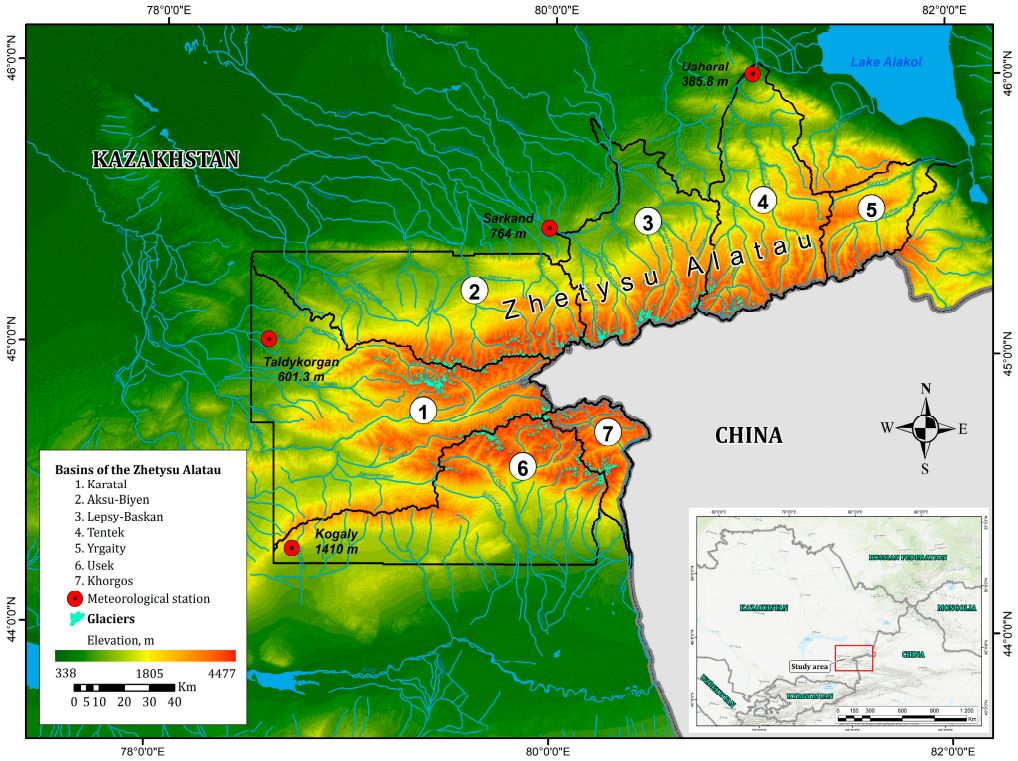

Figure 1. An overview map with the boundaries of the basins and the weather station.

The climate of the Zhetysu Alatau is mainly continental. It is under the influence of arctic, polar, and tropical air masses, which undergo significant transformation on the way. Arctic air masses come from the north and northwest, from the Barents and Kara seas. They come mostly in the first half of the winter period. Their invasion is accompanied by a sharp drop in air temperatures.

The average long-term air temperature in the lower part of the glacial zone (at altitudes of 3200–3600 m) during the accumulation period is −8–−10 °C; in the upper part (above 4000 m), it drops to −14–−16 °C. As the terrain rises above sea level, differences in climatic conditions are clearly manifested. According to the climate references [25], the coldest month is January, the temperature of which ranges from −7.5 at meteorological station (MS) Sarkand to −13.2 °C (MS Usharal). The warmest month is July, when the temperature reaches 24.3 °C in the foothill areas and 17.7 °C in the mountains. The region's climate is characterized by well-developed temperature inversions, i.e., the temperature increases with elevation. The minimum air temperatures drop to an average of −18.3 °C in the flat areas and −13.4 °C in mountainous areas. The absolute minimum reaches −44 °C, and the absolute maximum is 44 °C. The warm season, with a mean daily air temperature above 0°, varies from 116 days to 137 days in mountainous areas. The duration of the frost-free period in most of the territory is 123–161 days. Spring frosts stop mainly at the end of

April (23–29 April), and the first autumn frosts in most areas are observed at the end of September and the beginning of October.

The annual rainfall is from 298 mm to 520 mm in the mountains. In the warm season of the year (from April to October), 50–65% of the annual precipitation falls. The average annual wind speed is 1.1–2.7 m/s. Steady snow cover is observed in late November–early December. The snow cover melting is observed in the end of March. The duration of the stable snow cover is 111–155 days. The average of the maximal heights of snow cover does not exceed 15–33 cm during winter [26].

3. Materials and Methods

3.1. Utilized Images

We used data from optical satellites such as Landsat ETM+ and Landsat OLI. We also used high-resolution imagery from Google Earth (QuickBird satellite) to define glacier contours in difficult areas and assess the mapping accuracy. We selected only two observation months (10 August to 25 September) due to minimal snow cover. The scenes were taken on cloudless days of this period, but some of the edges of the glaciers were hidden by shadows from the rocks and the walls of the glacial cirque. In total, six Landsat 7 (ETM+) scenes were used for 2001–2012, and three Landsat 8 (OLI) scenes for 2015–2016.

Landsat (level L1T) georeferenced imagery was provided by the USGS Center for Earth Observation and Science (EROS) (http://earthexplorer.usgs.gov/ (accessed on 20 December 2020)). A panchromatic channel with a resolution of 15 m was used to improve the quality of maps using the pan-sharpening tool (Table 1).

Table 1. List of images used in the study.

WRS2 Path-Row	Date	Satellite and Sensor	Spatial Resolution (m)	Suitability of Scenes	Suitability of Scenes
148-029	22 August 2001	Landsat ETM+	15/30/60	Main	
147-029	18 August 2002	Landsat ETM+	15/30/60	Additional information	Seasonal snow
147-029	12 September 2011	Landsat ETM+	15/30/60	Additional information	Filling the gaps
148-029	3 September 2011	Landsat ETM+	15/30/60	Additional information	Filling the gaps
147-029	13 August 2012	Landsat ETM+	15/30/60	Main	
148-029	20 August 2012	Landsat ETM+	15/30/60	Main	
147-029	1 September 2016	Landsat OLI	15/30/60	Main	Seasonal snow, shadow areas
148-029	24 September 2016	Landsat OLI	15/30/60	Main	Seasonal snow, shadow areas
148-029	21 August 2015	Landsat OLI	15/30/60	Additional information	Shadow areas

Due to the unfavorable natural and climatic characteristics of the Landsat 7 ETM+ images for 2001, covering the eastern part of the Zhetysu Alatau, an additional image from the Landsat 7 ETM+ satellite of 2002 was used.

Since Landsat 8 OLI was only launched in 2013, and the Scan Line Corrector (SLC) in the ETM+ instrument (Landsat 7) failed in 2003, the 2012 ETM+ images required preprocessing, namely the Gap filling process, that is, filling in the missing pixels. This procedure was carried out in the ENVI software using the Gap Fill module. The images from 2012 were used as the "master file", and the images from 2011 were used as the "slave file" (Figure 2).

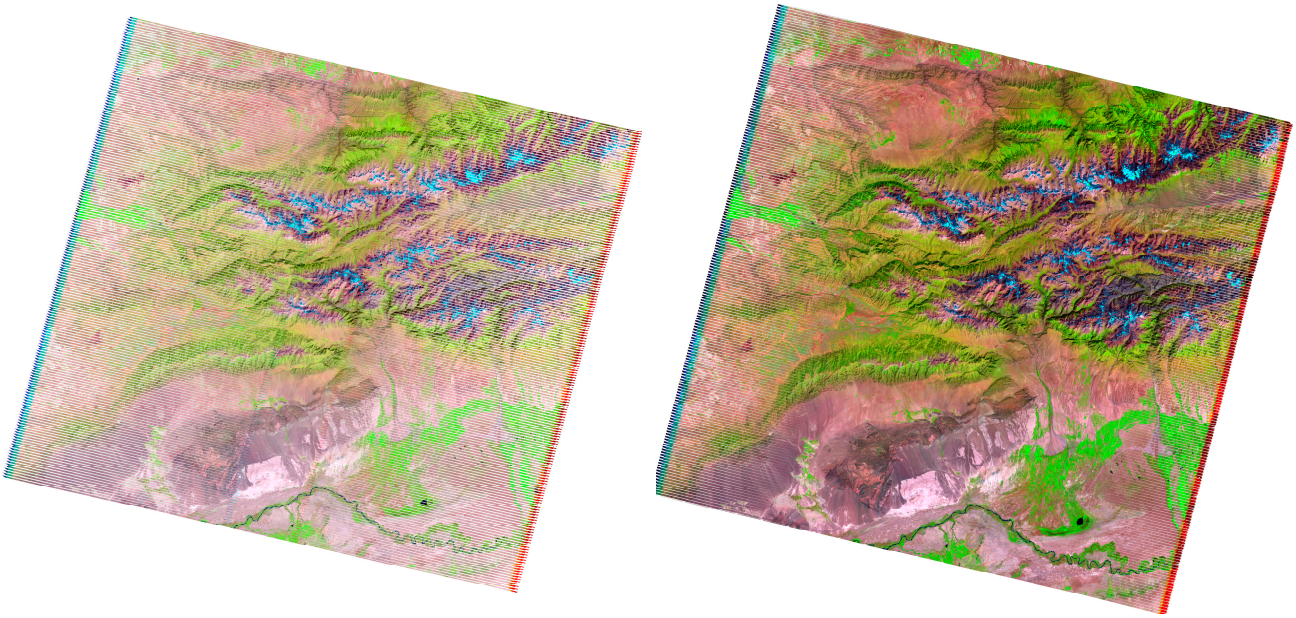

before after

Figure 2. Filling gaps in the Landsat ETM+ (2012).

In addition to the 2016 Landsat OLI satellite images, the 2015 Landsat OLI images were used due to improved shadow conditions, which in turn allowed more detailed mapping of the glaciers.

The satellite imagery available on Google Earth for glacier contouring served as a visual guidance tool, with data coming primarily from very-high-resolution optical sensors (Google Earth 2017). Unfortunately, it was not available for all study areas.

The ALOS PALSAR DEM was used to extract watersheds and topographic information for the glacier inventory. For the dynamics of the glacier areas, we analyzed the 2nd edition of the 13th volume of the *Catalog of Glaciers of the USSR* (*Glaciers On The Territory of Zhetysu Alatau*) 1969, 1970, 1975, and 1980, published on the basis of aerial photographs of 1956.

3.2. Climatic Data

An assessment of the dynamics of spatial and temporal changes in the amount of precipitation and temperature indicators in the study area was carried out on the basis of long-term observation data analysis of the Usharal, Taldykorgan, Sarkand, and Kogaly meteorological stations (according to the *Manual on the Global Observing System. Volume I—Global Aspects*, World Meteorological Organization 2015 (WMO-No. 544) observations at the meteorological stations of the RSE "Kazhydromet", carried out every three hours at the main standard (00:00, 06:00, 12:00, and 18:00) and intermediate times (03:00, 09:00: 00, 15:00, and 21:00)). Detailed information about the mentioned meteorological stations is illustrated in Table 2.

We also used data from the Republican Hydrometeorological Fund RSE "Kazhydromet" for the period from 1960 to 2021. A constant upward trend in the mean temperatures was observed throughout Kazakhstan. According to Cherednichenko et al., 2015 [27], the increase in the average annual air temperature is 0.32 °C every decade in Kazakhstan. Atmospheric precipitation demonstrated a slight upward trend (by 2.6 mm/10 years), mainly due to spring period precipitation, when the increase in some western and northern regions is 10–20%/10 years. In autumn, the precipitation amounts decrease in some western and southern regions by 2–12%/10 years. All trends in the average annual and seasonal precipitation are statistically negligible all over Kazakhstan.

Table 2. Geographic location of selected weather stations.

	Meteorological Stations (MSs)	Elevation (m)	Coordinates	Description
1	Usharal	385.8	46°10′N, 80°56′E	It is located in the desert plain region of the Alakol depression, Tentek river basin, eastern part of the Zhetysu Alatau.
2	Taldykorgan	601.3	45°01′N, 78°22′E	It is located in the foothill region of the western Zhetysu Alatau (Karatal river basin).
3	Sarkand	764	45°25′N, 79°55′E	It is located on the northern part of the Zhetysu Alatau (Lepsy river basin).
4	Kogaly	1410	44°29′N, 78°39′E	It is located on the southern part of the Zhetusy Alatau (Usek river basin).

The most recommended and useful methods for determining trends in climate change are nonparametric methods [28]. Therefore, for the assessment of the general trend in changes in air temperature and precipitation, we used the nonparametric statistical method of Mann–Kendall with a *p*-value of 95%. The calculations were carried out in the R program in the mk.test[2] application. The test detects any upward or downward trends in the time series data. If the *p*-value is less than the significance level α (alpha) = 0.05, it indicates the presence of a trend in the time series, i.e., the result is statistically significant; if the *p*-value is greater than the significance level, this indicates that the trend has not been detected.

In addition, the analysis of change tendencies in the characteristics of the climatic regime for the study period was carried out on the basis of calculated linear trends in the series of observations using the least squares method.

3.3. Methods

F. Paul [29,30] compared the different methods, including the band ratios of Landsat ETM +(3/5, 4/5) and Landsat OLI (4/6, 5/6), including filters and mapping in shadow areas [31]. According to his study, the ratio of Landsat ETM + (TM 3/5) and Landsat OLI (OLI 4/6) is the most reliable, reproducible, and simple method, in parts even better than manual mapping. Furthermore, this method has been applied by various authors to glaciers around the world [32].

In this regard, we used a semiautomatic method based on the ratio of bands (Figure 3a). The technique is based on using the threshold ratio values of the spectral channels of optical images (Landsat, Sentinel-2) to determine the contour of a glacier. We used the RED/SWIR-1 channels of the Landsat satellite. The threshold value of 2.1 was set manually through visual inspection (the clean-ice and snow patch). To clean up the glacier polygon, we used a median filter (3 by 3 kernel size) (Figure 3b) and then converted it to a vector (Figure 3c).

For mapping glaciers in the shadow areas, we used Band 2 (Blue) with threshold 7400 (set manually by visually checking). For mapping all shadow areas, we applied SRTM HillShade, which calculated using sun azimuth and other parameters, as in Landsat imagery metadata. We obtained glaciers in shadow areas as the intersection of Band 2 > 7400 and Hillshade $\leq$ 0 (less than or equal to 0) (Figure 3d).

Additionally, the delineation of the glacier tongue, covered with debris, was performed using additional data, such as thermal band and geomorphological characteristics obtained from the DEM, as well as Google Earth images. However, debris cover was not a major problem in defining the glacier boundaries, due to the fact that most of the glacier surface in this area is pure ice.

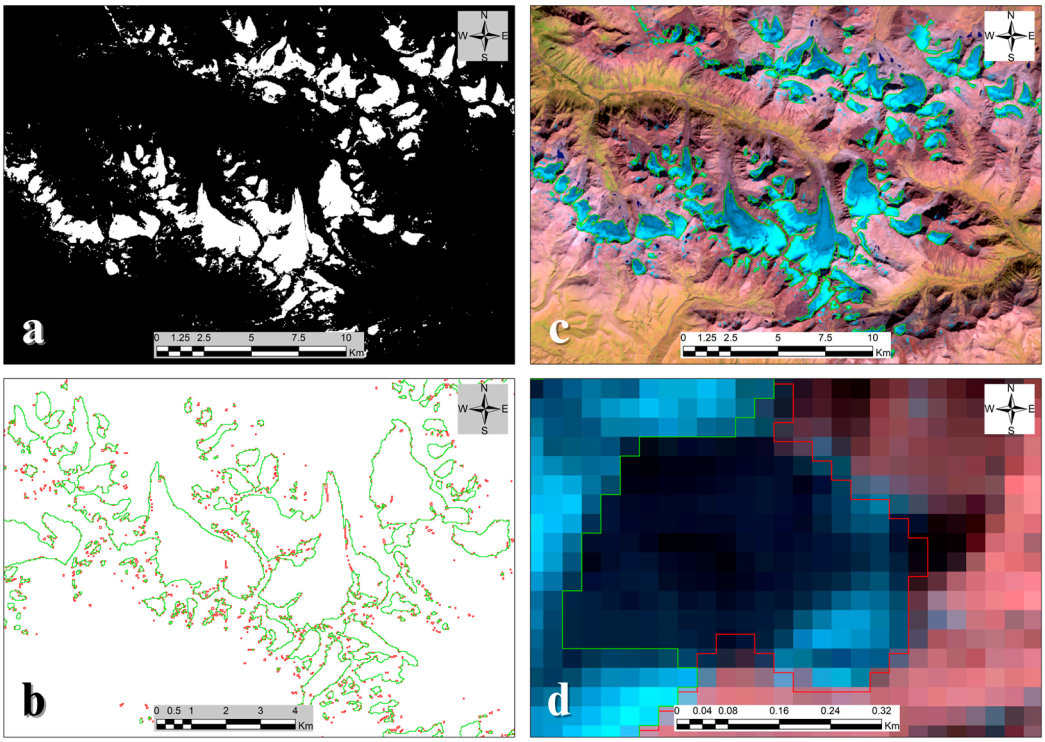

Figure 3. Glacier mapping using a semiautomated band ratio technique: (**a**) TM3/TM5, OLI4/OLI6; (**b**) after filtering (median filter 3 × 3); (**c**) raster to vector format conversion; (**d**) mapping of glaciers in the shadow area.

3.4. Uncertainty of Mapping

In order to correctly interpret and estimate the importance of the study, the accuracy needs to be evaluated. In our previous study [13], uncertainty was estimated with the buffer method [33,34]. The size of the buffer was chosen to be half of the estimated RMSE, i.e., 7.5 m to each side, and the accuracy was within ±5% for our study region.

We also determined uncertainty using another independent way, namely, the multiple digitization of glacier outlines, which is the best method to define the accuracy of mapping by one analyst [34]. This method gives the most realistic (analyst-specific) estimate for the provided dataset. Despite the higher workload, this method is recommended for use instead of the literature value or buffer methods. Following Paul et al. (2013) [29], we manually digitized four glaciers five times (one time every day) independently, using a reference dataset with high resolution (Figure 4). Then, the resulting average areas were compared with the area obtained automatically using TM. As a result, the difference between the manually and automatically derived area was around 1–3.5 and 2–4.5%, respectively (Table 3).

Table 3. Comparison of glacier area values.

Glaciers	Manually Delineated							Automated with TM. km²	Std%	Diff%
	1 Day	2 Day	3 Day	4 Day	5 Day	Mean. km²	Mean-koef. km²			
a	1.4356	1.4085	1.4271	1.4193	1.4302	1.4241	1.4105	1.3958	2.0	1.4
b	2.7081	2.7114	2.7147	2.7275	2.7253	2.7174	2.6913	2.6621	2.0	1.0
c	4.1658	4.1790	4.1970	4.2279	4.2338	4.2007	4.1604	4.0848	2.8	3.4
d	0.3853	0.3860	0.3877	0.3941	0.3923	0.3891	0.3853	0.3716	4.5	4..0

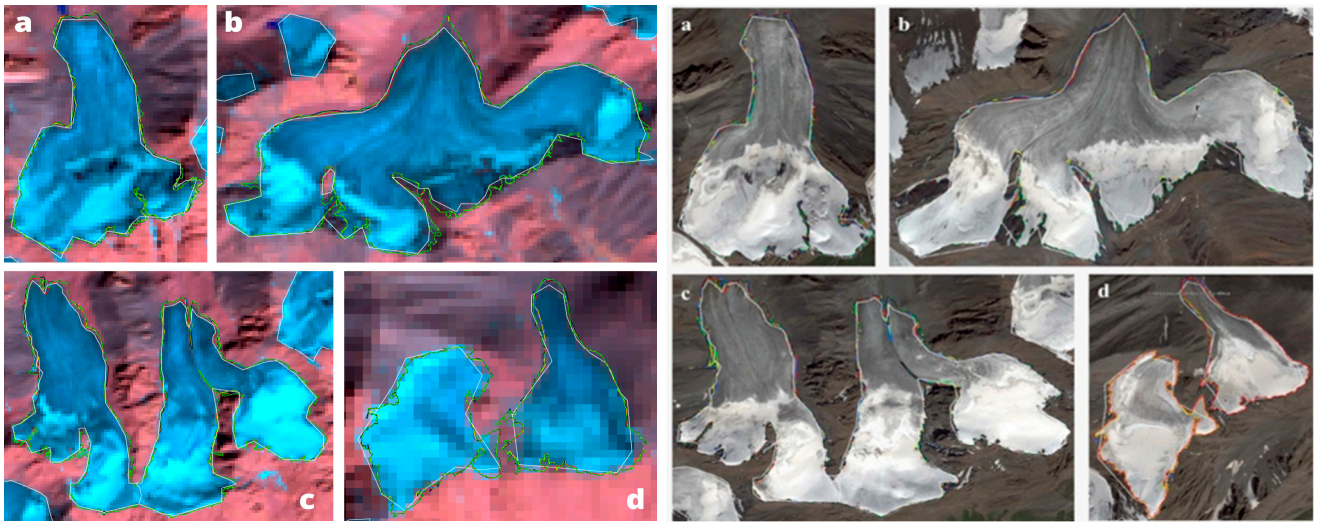

Figure 4. Overlay of four (**a**–**d**) manually digitized glacier extents (colored) and the white outline is derived automatically from TM: (**I**) on the Landsat 8 OLI images; (**II**) on the Google Earth images.

4. Results

4.1. Glacier Inventory of 2001

According to Landsat data for 2001, we identified and mapped 897 glaciers with an area of more than 0.005 km^2 each, with a total area of 517.4 ± 14.5 km^2 in the basins of 7 large rivers (including sub-basins) of the Zhetysu Alatau (Table 4). Of these, 126.5 ± 3.5 km^2 or 24.4% of the total area of glaciers falls on the western part (Karatal) of the Zhetysu Alatau, 197.2 ± 5.5 km^2 or 38.1% on the northern part (Aksu-Bien and Lepsy-Baskan), 59.7 ± 1, 7 km^2 or 11.5% on the eastern part (Tentek and Rgayty), and 133.9 ± 3.7 km^2 or 26% was found in the southern part (Khorgos and Usek) (Figure 5).

Table 4. Glacier area change.

Basins	1956	2001	2012	2016	1956–2001	2001–2012	2012–2016	2001–2016	1956–2016	Mean Size in 2001/2016
	Area km^2 (Count)				Area Decrease % (% yr^{-1})					
1	2	3	4	5	6	7	8	9	10	11
Karatal	202.5 (285)	126.5 ± 3.5 (231)	110.3 ±3.1 (221)	102.6 ± 2.9 (220)	−37.5 (0.8)	−12.8 (−1.2)	−7 (−1.7)	−18.9 (−1.3)	−49.3 (−0.8)	0.55/0.47
Aksu Bien	140.4 (135)	93.4 ± 2.6 (133)	83.1 ± 2.3 (127)	77.1 ± 2.2 (127)	−33.5 (−0.7)	−11 (−1)	−7.2 (−1.8)	−17.5 (−1.2)	−45.1 (−0.8)	0.70/0.60
Lepsy-Baskan	154 (116)	103.8 ± 2.9 (112)	93.7 ± 2.6 (111)	88.4 ±2.5 (105)	−32.6 (−0.7)	−9.7 (−0.9)	−5.7 (−1.4)	−14.9 (−1)	−42.6 (−0.7)	0.91/0.83
Tentek	75.2 (94)	49.7 ± 1.4 (85)	41.8 ± 1.2 (73)	36.9 ± 1.0 (58)	−33.9 (−0.8)	−15.8 (−1.4)	−12.6 (−3.1)	−26.4 (−1.8)	−51.4 (−0.9)	0.57/0.63
Rgaits	13.1 (22)	10 ± 0.3 (21)	8.2 ± 0.2 (18)	6.9 ± 0.2 (17)	−23.5 (−0.5)	−18.4 (−1.7)	−16.2 (−4.1)	−31.6 (−2.1)	−47.7 (−0.8)	0.47/0.40
Usek	144.8 (233)	84.9 ± 2.4 (219)	73.4 ± 2.1 (202)	64.6 ± 1.8 (197)	−41.4 (−0.9)	−13.6 (−1.2)	−12 (−3)	−23.9 (−1.6)	−55.4 (−0.9)	0.38/0.32
Khorgos	83.5 (100)	49 ± 1.4 (96)	43.2 ± 1.2 (90)	38.5 ± 1.1 (89)	−41.3 (−0.9)	−11.9 (−1.1)	−11 (−2.7)	−21.6 (−1.4)	−53.9 (−0.9)	0.51/0.43
Total	813.6 (985)	517.4 ± 14.5 (897)	453.7 ± 12.7 (842)	414.6 ± 11.6 (813)	−36.4 (−0.8)	−12.3 (−1.1)	−8.6 (−2.2)	−19.9 (−1.3)	−49 (−0.8)	0.57/0.51
Glaciers <0.005 km^2	18.9 (385)	5.1 ± 0.14 (143)	3.7 ± 0.10 (96)	3 ± 0.08 (83)	−72.9 (−1.6)	−27.4 (−2.5)	−19.3 (−4.8)	−41.4 (−2.8)	−84.1 (−1.4)	0.04/0.03

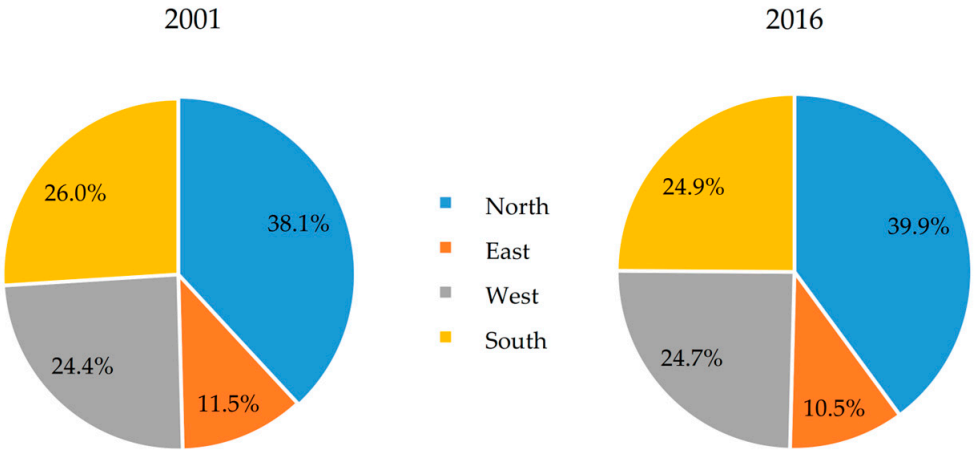

Figure 5. Glacier distribution in the Zhetysu Alatau between regions.

The average size of the glaciers for the entire mountainous region was 0.57 km^2, with the glaciers of the 1.0–5.0 km^2 size class prevailing, with a total area of 221.5 ± 6.2 km^2 (Figure 5), which is 42.8% ± 2.8 of the total area. Of these, 38% ± 2.8 was concentrated in the northern part (the basins of the Aksu-Bien and Lepsy-Baskan rivers) of the Zhetysu Alatau.

The larger glacier sizes (0.7–0.91 km^2) were concentrated in the northern part of the Zhetysu Alatau (the basins of the Lepsy-Baskan and Aksu-Bien rivers), while the average sizes of the glaciers in the southern (Usek) (0.38 km^2) and eastern part (Rgayty—0.47 km^2) were smaller (Table 4).

Glaciers with a size class of 0.1–0.5 km^2 were the most numerous (381 glaciers) in 2001 (Figure 6b).

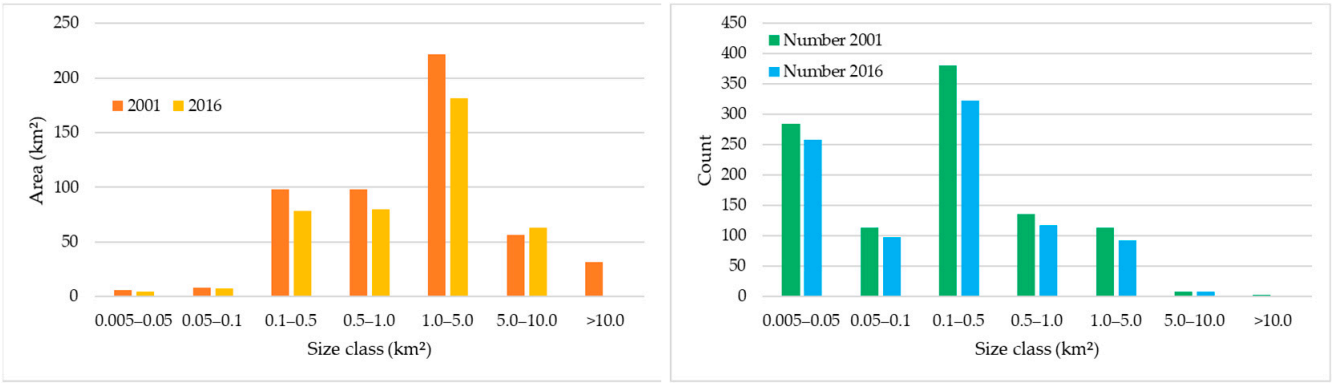

(**a**) (**b**)

Figure 6. Dynamics of glaciers: area (**a**); number (**b**) changes for seven size classes in the Zhetysu Alatau in 2001 and 2016.

Most glaciation areas of the Zhetysu Alatau faced north (north, northwest, and northeast) (Figure 7a,b) and were located at altitudes between 3000 and 4000 m.a.s.l. (Figure 8).

Glaciers with northern, northeastern, and northwestern exposure were the most extensive in the Zhetysu Alatau, covering 163.55 ± 4.6 km^2, 121.32 ± 3.4 km^2, and 105.48 ± 3 km^2, respectively, and they accounted for 75.4 ± 2.8% of all glaciers (Figure 7b). The southern, southeastern, and southwestern sides occupied 13.61 ± 0.4 km^2, 20.96 ± 0.6 km^2, and 14.72 ± 0.4 km^2, respectively, and together, they accounted for 9.5 ± 2.8% of all glaciers. The western side occupied 32.27 ± 0.9 km^2, or 6.1 ± 2.8%, and the eastern side, 47.20 ± 1.3 km^2, or 9%, respectively (Figure 7b).

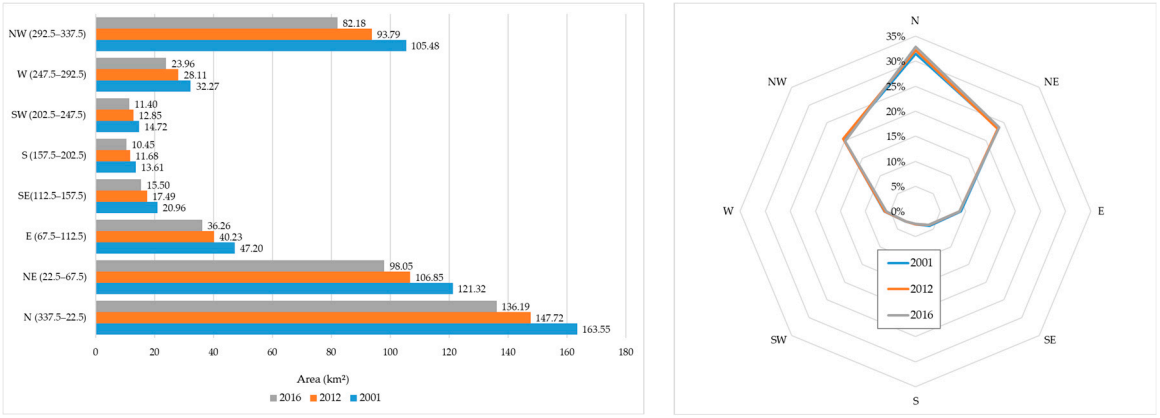

Figure 7. Glacier area change distribution by exposition in the Zhetysu Alatau in 2001, 2012, and 2016: (**a**) area, km^2; (**b**) area, (%).

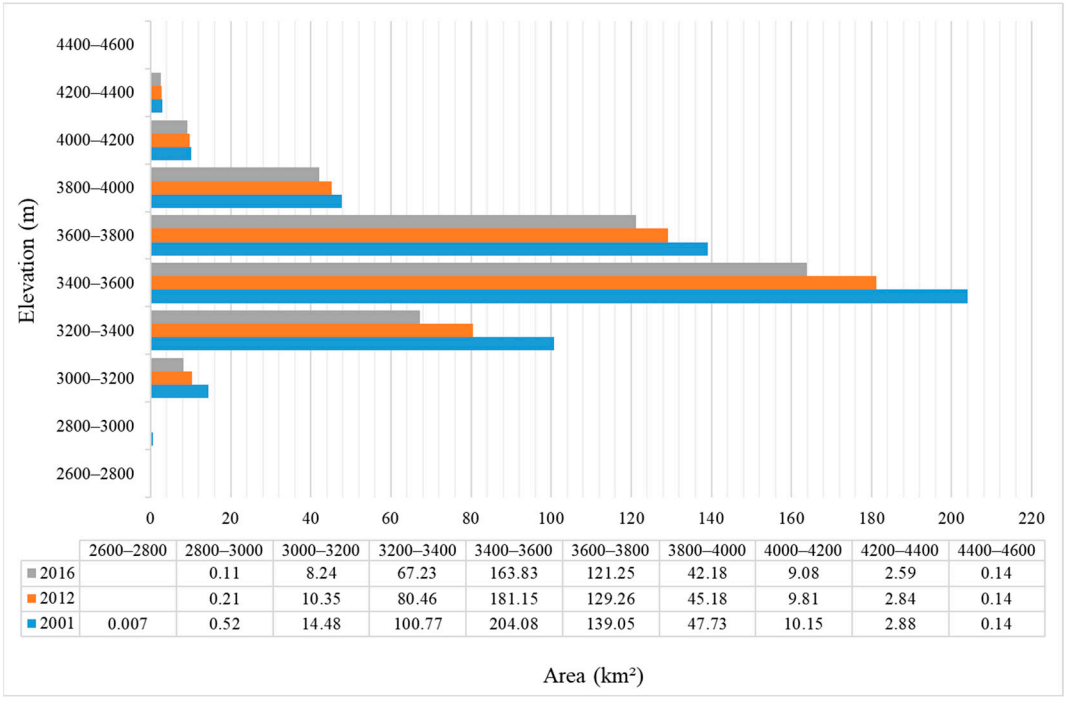

	2600–2800	2800–3000	3000–3200	3200–3400	3400–3600	3600–3800	3800–4000	4000–4200	4200–4400	4400–4600
2016		0.11	8.24	67.23	163.83	121.25	42.18	9.08	2.59	0.14
2012		0.21	10.35	80.46	181.15	129.26	45.18	9.81	2.84	0.14
2001	0.007	0.52	14.48	100.77	204.08	139.05	47.73	10.15	2.88	0.14

Figure 8. Glacier area distribution and changes by elevation in the Zhetysu Alatau in 2001, 2012, and 2016.

About 39.4 ± 2.8% of the glaciers of the Zhetysu Alatau were located at altitudes of 3400–3600 m, almost 26.9% at altitudes of 3600–3800 m and about 19.5 ± 2.8% at altitudes of 3200–3400 m (Figure 8).

In 2001, according to Landsat data, three glaciers with an area greater than 10 km^2 were identified and mapped in the Zhetysu Alatau. Two of them were located in the northern part (in the Lepsy river basin) of the Kolesnik glacier (10.3 ± 0.3 km^2) and Bereg (10.9 ± 0.3 km^2), and one in the western part (in the Karatal river basin) of the Bezsonov glacier (10.3 ± 0.3 km^2).

4.2. Glacier Inventory of 2016

In 2016, 813 glaciers with a total area of 414.6 ± 11.6 km^2 were identified and mapped in the Zhetysu Alatau (Table 4). Of these, 102.6 ± 2.9 km^2 or 24.7 ± 2.8% of the total area of glaciers falls on the western part (Karatal) of the Zhetysu Alatau, 165.5 ± 4.6 km^2 or

39.9 ± 2.8% on the northern part (Aksu-Bien and Lepsy-Baskan), 43.8 ± 1, 2 km^2 or 10.5% in the eastern part (Tentek and Rgaity), and 103.1 ± 2.9 km^2 or 24.9 ± 2.8% was found in the southern part (Khorgos and Usek) (Table 4, Figure 5).

In 2016, glaciers with a size of 1.0–5.0 km^2 (181.2 ± 5 km^2 ~ 43.7 ± 2.8%) predominated in terms of total occupied area, and glaciers with size of 0.1–0.5 km^2 predominated in number (322 glaciers). However, the area of glaciers from the group of 5.0–10.0 km^2 increased, and there were no glaciers with an area of more than 10 km^2 in 2016 in the Kazakhstan part of the Zhetysu Alatau (Figure 6a).

The average height of glaciers ranged from 3580 m above sea level (northern slope) to 3640 m (southern slope); on average, the glacier location was at an altitude of 3615 m above sea level. Most glacier areas (316.9 ± 8.9 km^2) in 2016 belonged to northern exposure slopes (N, NW, and NE), while the relative number and areas of glaciers facing the southern exposure parts (S, SW, and SE) were very small (Figure 7a,b).

The glacier ends were located at a mean minimum height of 3407 m.a.s.l., and their average maximal height was at 3746 m.a.s.l. Figure 9a illustrates the distribution of glacier area by the maximum and minimum heights. This means that large valley glaciers have a lower tongue and smaller glaciers have a higher tongue [13]. Additionally, Figure 9b illustrates the spatial spreading of the average height of glaciers greater than 0.01 km^2 in 2016.

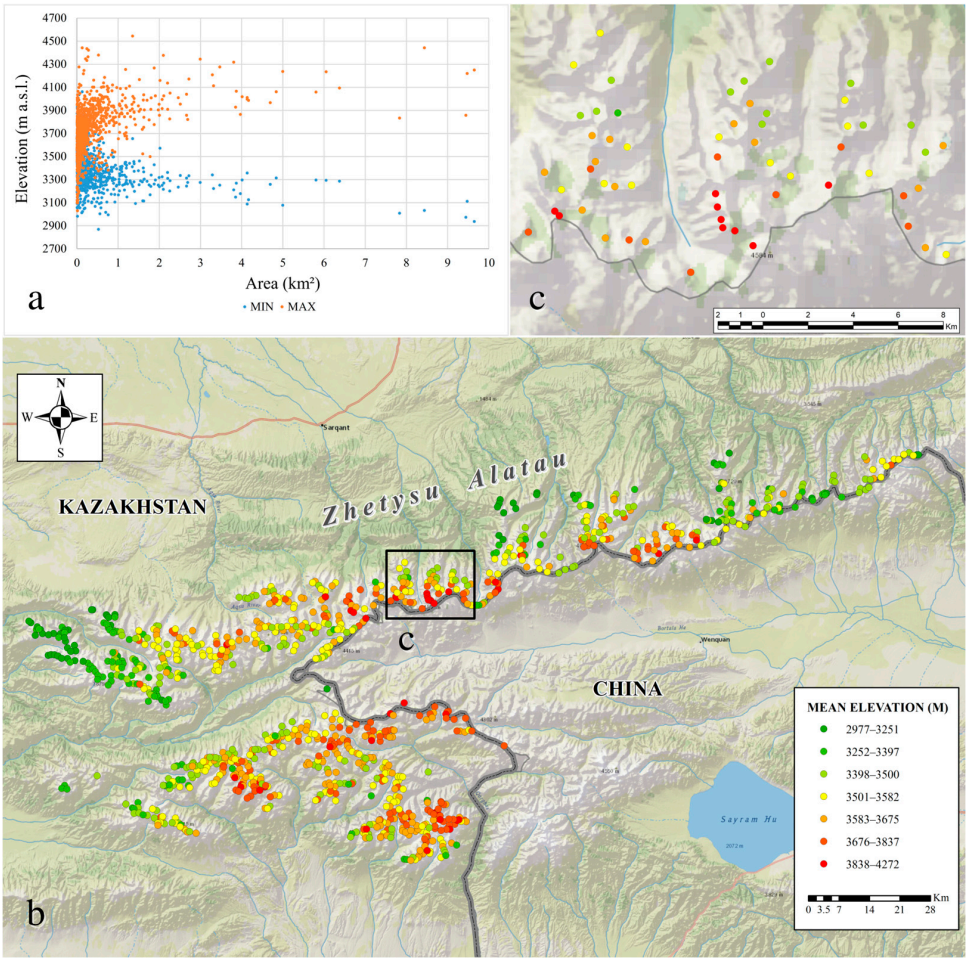

Figure 9. Corresponding distribution of glaciers of Zhetysu Alatau in the maximum and minimum altitude zones: (**a**) distribution of glacier area by the maximum and minimum heights; (**b**) distribution map of the glaciers average height; (**c**) an enlarged example of glaciers distribution by mean elevation in the selected area.

In 2016, there were three large glaciers along the Zhetysu Alatau with a total area of 28.6 km^2. Two of them were the Kolesnik (9.6 ± 0.3 km^2) and Bereg (9.5 ± 0.3 km^2) glaciers in the northern part (in the Lepsy river basin) and Bezsonov (9.4 ± 0.3 km^2) in the western part (in the Karatal river basin). As we have already noted, in 2016, there was no glacier with an area greater than 10 km^2 along the Zhetysu Alatau.

4.3. Glacier Changes in 2001–2016

As a part of this study, 897 glaciers were identified in 2001 and 813 in 2016, which were listed in the glacier catalog with a total area of 517.4 ± 14.5 and 414.6 ± 11.6 km^2, respectively (Table 4). The study results demonstrate that changes in the glacier areas of the Zhetysu Alatau had a significant decrease during the period from 2001 to 2016. Between 2001 and 2016, the total loss of glaciers was 102.8 ± 2.9 km^2 or 19.9 ± 2.8% (−1.3% yr^{-1}).

The highest rates of shrinkage of the glacier area were in the eastern (Rgaity and Tentek) and southern (Usek and Khorgos) parts of the Zhetysu Alatau.

For the period 2001–2016, the glacier area decreased by 31.6 ± 2.8% (−2.1% year^{-1}) from 59.7 ± 1.7 km^2 to 43.8 ± 1.2 km^2 in the eastern part, i.e., in the Rgaity river basin, and by 26.4 ± 2.8% (−1.8% year^{-1}) in the Tentek river basin.

The reduction rate of glacier areas in the northern (Aksu-Bien and Lepsy-Baskan) and western (Karatal) parts of the Zhetysu Alatau was relatively low. Between 2001 and 2016, the glacier areas belonging to the Karatal river basin (western) decreased by 18.9 ± 2.8% (−1.3% year^{-1}), in the Aksu-Bien rivers (northern), this shrinkage was 17.5 ± 2.8% (−1.2% yr^{-1}). The smallest reduction in the glacier area in the Zhetysu Alatau was noted in the Lepsy-Baskan river basin, belonging to the northern part. Between 2001 and 2016, the glacier area in this basin decreased by 14.9 ± 2.8%, and the annual reduction rate was 1% per year.

The average size of the Zhetysu Alatau glaciers in 2001 was 0.58 km^2, while in 2016, the average size decreased by 0.51 km^2. There was a decrease in the average size of glaciers in all areas; however, only the glaciers of the Tentek river basin (eastern part) increased from 0.57 km^2 to 0.63 km^2 on average. This happened due to the shrinking of small glaciers in the basin. As an example, in 2001, there were 90 glaciers in the Tentek river basin with a total area of 11.1 km^2 up to 0.5 km^2 in size, and in 2016, their total area was 5.7 km^2—almost halved—and 45 glaciers remained.

The analysis of the relative change in area compared to the initial area of the glacier indicated a large relative loss of smaller glaciers (from 0.01 to 0.1 km^2) (Figure 10). For larger glaciers (>1.0 km^2), the loss factors were smaller and more similar. The difference in shrinkage rate between the northern and western slopes was insignificant.

However, there were wide variations in losses, especially for smaller glaciers, while there were also glaciers of all size classes that only slightly decreased. The total area loss was higher for larger glaciers, and the average glacier height increased by 24 m, while the average minimal glacier height increased by 42 m from 3367 to 3409 m.a.s.l. over the period 2001–2016.

4.4. Temperature and Precipitation Trends

The resulting estimates of air temperature trends showed that the temperature increase occurred at all stations in all seasons and months of the year. However, there were some peculiarities in the rate of air temperature increase (Table 5). The table shows that the most noticeable increase in the average annual temperature was in the desert plain zone of the Alakol depression (MS Usharal), and the average rate of change was 0.29 °C/10 years. The lowest rates of temperature change were observed in the mountainous regions of the Zhetysu Alatau (0.12 °C/10 years—MS Kogaly). The trends in summer temperatures (June–August) showed that in mountainous and foothill areas, they had the highest values and ranged from 0.19 °C/10 years (MS Kogaly) to 0.25 °C/10 years (MS Taldykogan), and the lowest were at Usharal MS (0.12 °C/10 years). An analysis of changing trends showed that a steady increase in air temperature has been observed in the study area in recent

decades; the only exception was the Sarkand MS, where a slight decrease in precipitation was found. At the same time, in 2019 and 2020, at the three MSs of Taldykorgan, Usharal, and Kogaly, there was a deficit in atmospheric precipitation. At the same time, the smallest anomalies were observed at the MS Usharal (12–64 mm), and the largest was observed at the mountain station of Kogaly, 183 mm, which is 65% of the norm.

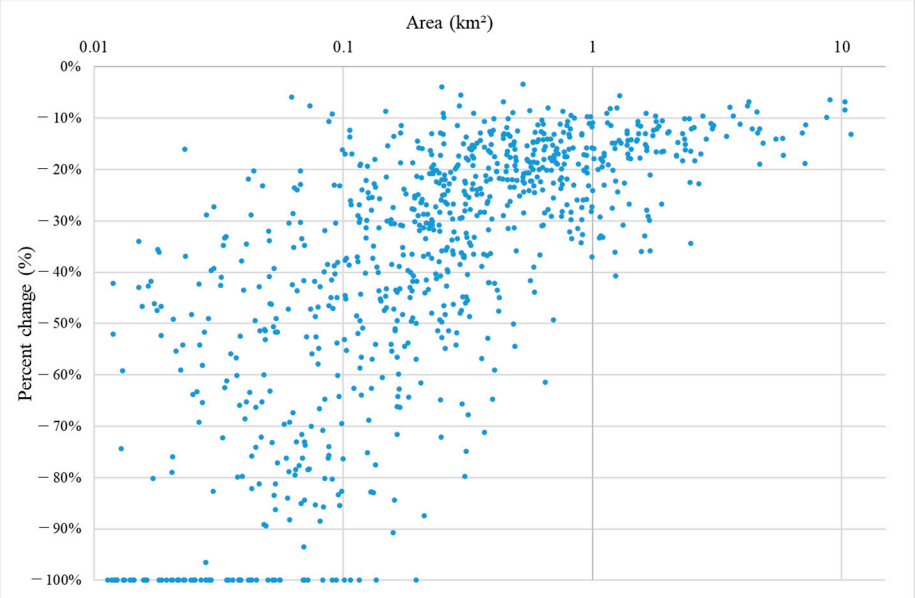

Figure 10. Scatterplot of relative glacier changes compared to initial glacier size for 813 glaciers between 2001 and 2016.

Table 5. Average annual and summer rates of change in air temperature (°C/10 years) and precipitation (mm/10 years) in 1960–2021.

No.	Meteorological Stations	Average Annual Rate of Air Temperature Change °C/10 Years	Average Summer Air Temperature Change Rate °C/10 Years	Average Annual Rate of Change in Precipitation, mm/10 Years
1	Taldykogan	0.28	0.25	8.5
2	Kogaly	0.18	0.19	9.3
3	Usharal	0.20	0.20	−2.2
4	Usharal	0.29	0.12	11.4

Thus, in contrast to the air temperature, the change in the precipitation regime in the study area gives a more variegated picture. The time series of annual precipitation anomalies for the period 1960–2021 give a general idea of the nature of modern changes in the precipitation regime. There have been no long-term trends over the last 40 years; there was an alternation of short periods with positive and negative anomalies in the amount of precipitation.

The significance of trends for both air temperature and precipitation was assessed for the summer months, as well as for the average annual and summer periods. An analysis of the data in Tables 6 and 7 showed that there was a significant upward trend in the average annual temperature in the study area. This was confirmed by the nonparametric Mann–Kendall statistic, which gave a positive Z-statistic. The average annual values of Z-statistics for air temperature reached 4.2276 (MS Usharal).

Table 6. Mann–Kendall statistics of average annual and summer (June–August) air temperatures for the study area.

Station	Mann–Kendall Stats	June	July	August	Mean Summer Period (June–August)	Annual Mean
Air Temperature						
Taldykorgan	Z-statistic	2.9339	3.0857	3.7235	3.8145	3.7295
	p-value	0.003347	0.002031	0.0001965	0.0001364	0.0001919
	Significance	(**)	(**)	(***)	(***)	(***)
Kogaly	Z-statistic	2.8003	2.7152	2.6483	3.5837	4.2033
	p-value	0.005106	0.006623	0.00809	0.0003388	0.00002631
	Significance	(**)	(**)	(**)	(***)	(***)
Sarkand	Z-statistic	2.8913	2.1745	2.2596	3.4379	3.2132
	p-value	0.003836	0.02967	0.02385	0.0005862	0.001312
	Significance	(**)	(*)	(*)	(***)	(**)
Usharal	Z-statistic	2.1138	1.0508	1.6219	2.4418	4.2276
	p-value	0.03453	0.2933	0.1048	0.01462	0.00002362
	Significance	(*)	N.S.	N.S.	(*)	(***)

***: $\alpha = 0.001$; **: $\alpha = 0.01$; *: $\alpha = 0.05$; $\alpha = 0.1$ level of significance; N.S.—nonsignificant.

Table 7. Mann–Kendall statistics of average annual and summer (June–August) values of atmospheric precipitation for the study area.

Station	Mann–Kendall Stats	June	July	August	Mean Summer Period (June–August)	Annual Mean
Precipitation						
Taldykorgan	Z-statistic	0.11541	0.40699	0.94162	0.69853	1.1116
	p-value	0.9081	0.684	0.3464	0.4848	0.2663
		(N.S.)	(N.S.)	(N.S.)	(N.S.)	(N.S.)
Kogaly	Z-statistic	0.48594	−0.31586	0.99015	0.84431	0.62564
	p-value	0.627	0.7521	0.3221	0.3985	0.5315
		(N.S.)	(N.S.)	(N.S.)	(N.S.)	(N.S.)
Sarkand	Z-statistic	−0.6378	0.14578	0.82617	−0.12149	−0.14578
	p-value	0.5236	0.8841	0.4087	0.9033	0.8841
		(N.S.)	(N.S.)	(N.S.)	(N.S.)	(N.S.)
Usharal	Z-statistic	0.90517	0.21867	0.49812	1.0995	1.7979
	p-value	0.3654	0.8269	0.6184	0.2715	0.07219
		(N.S.)	(N.S.)	(N.S.)	(N.S.)	(N.S.)

N.S.—nonsignificant.

The average annual trend changes were assessed as significant, since all values were less than *p*-value < 0.05. The same picture was observed in the summer period (June–August). However, if we consider the change in trends by month, there were some differences. Significant positive trends were noted at the three studied meteorological stations (Taldykorgan, Kogaly, and Sarkand); the *p*-values were significantly less than 0.05. At Usharal MS, there was a significant trend only in June; in June and August, the trends

were insignificant. The results obtained are consistent with the results obtained in the Ishfaq Farooq (2021) study. Ishfaq Farooq [14,35] studied the air temperature time series for Kazakhstan using the M-K statistical test. The results showed that there was a significant increase in the average annual temperature in Kazakhstan from 1970 to 2017.

The results of the Mann–Kendall test showed that there were no statistically significant linear trends in precipitation for the period under study, at almost all stations, although strong interannual variability was observed in the time course. Statistically insignificant trends were observed at Sarkand MS in the average annual and summer season, but negative trends were noted (Z-statistic: −0.12149 in summer; −0.14578 per year). Similar results were obtained for other regions of Kazakhstan by Talipova et al. (2021) [36] and Shahgedanova (2018) [37]. Thus, we can conclude that climate change for the study area was observed in the form of an increase in air temperature and statistically insignificant positive trends in changes in precipitation.

5. Discussion

An intensive reduction in glacier area was confirmed by many previous studies [2,4,6,10,15,20,24,32,38–45]. However, our results show rates of area reduction of about −0.8% a^{-1} for the period 1956–2001, and −1.3% a^{-1} for the period 2001–2016, which are the highest values among all the glacial zones of the world and Central Asia, including Altai and Pamir [6,33,36,37]. It is important to note that the rate of decline increased rapidly, and amounted to −0.8%, −1.1%, 2.2%, and −1.3% a^{-1} for the periods 1956–2001, 2001–2012, 2012–2016, and 2001–2016, respectively. If we compare the rate of reduction in the area of glaciers in the study area with other glacial regions of the world, then significant differences can be observed. For example, according to the studies by Tielidze and Wheate (2018) [46], the reduction in the area of glaciers in the Greater Caucasus over the period 1960–1986 amounted to 11.5% (−0.44% a^{-1}), and for 1986–2014, this figure was 19.5% (−0.69% a^{-1}). In the research by Tennant et al. (2012) [47], glacier reduction in the Canadian Rockies was −28.3% (−0.4% a^{-1}) in the period of 1919–1985, −7.6% (−0.5% a^{-1}) in the period of 1985–2001, and −9.9% (2.0% a^{-1}) in the period of 2001–2006. In the European Alps, according to Paul et. al. (2020) [48], the total glacier area shrunk from 2060 km^2 in 2003 to 1783 km^2 in 2015/16, i.e., by −13.2% (−1.1% a^{-1}).

However, the features of the geographical location of the Tien Shan mountain system, in particular the natural zone, as well as the climatic conditions, are significantly different from the above-mentioned mountain systems. That is, the mountain system is located in the arid and semiarid region of Central Asia, surrounded by deserts. In addition, the speed of acceleration is significantly higher compared to other ranges of the Tien Shan mountain system [5,15,39,40,42].

Such a significant reduction in the areas of glaciers is fully consistent with other studies, which found that the greatest area loss occurred primarily in the peripheral areas with low-altitude ranges [10,49]. The study by Aizen et al. (2006) [43], for 1977–2003 in the inner region of Tien Shan, and Narama et al. (2006) [44], for 1971–2002 in the western Tien Shan, indicated a glacial decrease of 8–9% or 0.26–0.29% a^{-1}, while glacier reduction in the peripheral ranges of the northern Tien Shan was remarkably faster. For example, in the Ile and Kungey Alatau, the glacier reduction speed was −0.73% a^{-1} for the period of 1955–1999 [32]. The southern part of the Zhetysu Alatau was studied by Kokarev and Shesterova (2014) [49]; the calculated rate was about −0.86% per year.

The glaciers of the outer Tien Shan receive the greatest amount of precipitation, and they are very sensitive to even the slightest temperature changes due to the high rate of mass transfer. On the contrary, the glaciers of the inner Tien Shan react to climate change with a longer delay, since the accumulation and, consequently, the mass turnover of predominantly cold glaciers are relatively small [10,50–53].

This may be due to the peculiarities of the geographical location of the Zhetysu Alatau, as well as the morphometric parameters of glaciers (the type and size of glaciers), the location along the altitudinal strip, and factors such as climate. An increase in air

temperature also has implications for snow cover, such as a decrease in snow amounts and an increasing intensity of snowmelt [2,54,55].

Regions with predominantly small glaciers are more sensitive to changes due to the shorter response time of glaciers to climate change [56,57]. It has also been reported that smaller glaciers with a large edge area-to-length ratio are shrinking faster than larger glaciers at the same rate of melt [58]. In the Zhetysu Alatau, the vast majority of glaciers are small, at less than 1 km^2 in size. Small glaciers cover more than half of the total area, which is common in midlatitudes.

An additional reason for the greater loss of area may be the lower height of the glaciers of the Zhetysu Alatau. An increase in mean annual temperatures without a significant increase in precipitation will shift the ELA about 150 m upwards per degree [59]. At low altitudes, this upward shift in the ELA increases the risk of the entire glacier area falling into the ablation zone (Figure 11). A reduction in glaciers was found at all altitudes of the study area during the study period. However, the greatest changes in the area were shown by glaciers lying on the slopes of the western and northwestern exposures. Most of the glaciers lying on the slopes of the southern exposures were outside the study area, but those that were not showed a noticeable reduction.

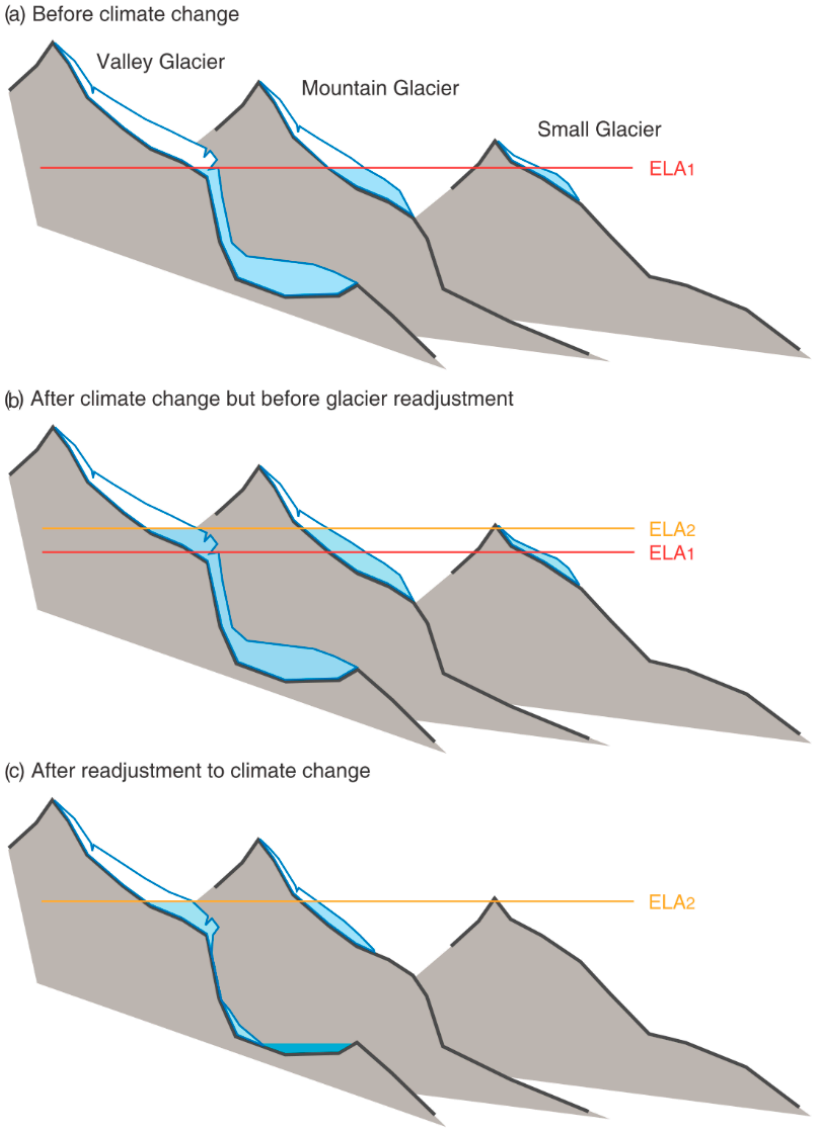

Figure 11. Schematic of the response of the three types of glaciers to climate change (from IPCC, 2013) [59].

Moreover, because of the western orientation, the Zhetysu Alatau ranges are also under the influence of warm western air masses originating over deserts located to the south of Lake Balkhash [54,60]. The exposure to moist air masses and dominating wind directions is strongly controlling the ELA elevation on ice [61]. Furthermore, the long-distance westerly winds are a carrier of fine-grained loess from the deserts of Central Asia to Tien Shan [60,62], polluting the glacial surfaces and intensifying the melting rate [59]. The frequency of dust storms directed to the Zhetysu Range has increased during the last few decades [62], so the shrinkage rate of our study area, located in the western Zhetysu Alatau, is almost three times as severe (−0.86% per year) as the Bortala River in the eastern Zhetysu Alatau (−0.32% per year) [63].

The rates of temperature change were observed in the mountainous areas of Zhetysu Alatau (Kogaly MS), where the average rate of change was 0.12 °C/10 years. The trends in summer temperature changes (June–August) showed that mountainous and foothill areas had the highest values, which ranged from 0.19 °C/10 years (Kogaly MS) to 0.25 °C/10 years (Taldykogan MS). A warming climate leads to increasing glacier melt and as well as less snow accumulation, which in turn causes a lower albedo in the glacier surface [63–65]. The upward trend in temperature caused an increase in rainfall rate rather than snowfall in the high-altitude zones, leading to a decrease in accumulation and an acceleration of ablation, especially during summer [65].

6. Conclusions

We have presented a new and updated catalog of glaciers for the Zhetysu Alatau range for the period of 2001–2016. Glaciers were detected in all seven river basins for the Zhetysu Alatau using Landsat satellite images from 2001 to 2016. With area loss rates of about −0.8% and −1.3% a^{-1} for the periods of 1956–2001 and 2001–2016, our results showed a higher rate than other regions of the Central Asian mountains, including Tien Shan, Altai, and Pamir. In addition, the rates of area shrinkage were significantly higher than other ranges of the Tien Shan mountain system, which were −0.8%, −1.1%, 2.2%, and −1.3% a^{-1} for the periods of 1956–2001, 2001–2012, 2012–2016, and 2001–2016, respectively.

For a more detailed analysis of the reason for the sharp reduction in the glacier, we analyzed climate data using the nonparametric Mann–Kendall test. Analyzing weather station climatic data, we found a significant increase in temperature at all stations. The trends in summer temperature changes (June–August) showed that mountainous and foothill areas had the highest values, ranging from 0.19 °C/10 years (Kogaly MS) to 0.25 °C/10 years (Taldykogan MS). An analysis of the trends in change showed that a steady increase in air temperature has been observed in the study area over the past decades.

It was found that climatic conditions play a main role in the state of glaciers. The location of the region under study on the periphery of the mountain system has less favorable conditions than the inner ranges. Moreover, a significant increase in temperature and a slight change in precipitation played a main role in the negative balance of glaciation in the Zhetysu Alatau.

Author Contributions: Conceptualization, S.N., A.K. and G.F.; methodology, S.N., A.K. and A.N.; software, K.Z., A.M. and S.N.; validation A.K. and S.N.; investigation, S.N., A.K. and K.Z; data curation, A.M., A.N., K.Z. and D.C.; writing—original draft preparation, K.Z., A.K. and N.S.; writing—review and editing, A.K., K.Z. and G.I.; visualization, A.M. and K.Z.; supervision, A.K.; project administration, A.K.; funding acquisition, A.K. All authors have read and agreed to the published version of the manuscript.

Funding: This research has been funded by the Science Committee of the Ministry of Education and Science of the Republic of Kazakhstan within the framework of the projects AP08856470 and AP14872134, and supported by the Postdoctoral Fellowship provided by Al-Farabi Kazakh National University. The APC was funded by the project budget.

Data Availability Statement: The Landsat ETM+ and Landsat OLI images used in this study can be downloaded from the United States Geological Survey at https://earthexplorer.usgs.gov/ (accessed on 20 December 2020). The Shuttle Radar Topography Mission (SRTM) 90 m DEM used in this study can be downloaded from CGIARCSI consortium for spatial information at https://cgiarcsi.community/ (accessed on 20 December 2020). The ALOS PALSAR 12.5 m DEM used in this study can be downloaded from the Alaska Satellite Facility at https://asf.alaska.edu (accessed on 20 December 2020). High-resolution optical images with 3D representation used in this study are available in the program Google Earth. *Glacier Inventory of the USSR* (1969, 1970, 1975, and 1980) is available at https://www.geokniga.org/books/ (accessed on 20 December 2020).

Acknowledgments: We are grateful to the providers of free data for this study: Alaska Satellite Facility (ASF), United States Geological Survey (USGS), and others. Thanks are due to DING Xiao-li, Chair Professor of Geomatics, Department of Land Surveying and Geo-Informatics, The Hong Kong Polytechnic University for his scientific consult and encouragement. We also acknowledge Baygurin Zhaksybek for his help during the preparation of the manuscript.

Conflicts of Interest: The authors declare no conflict of interest.

References

1. Barnett, T.P.; Adam, J.C.; Lettenmaier, D.P. Potential impacts of a warming climate on water availability in snow-dominated regions. *Nature* **2005**, *438*, 303–309. [CrossRef]
2. Sorg, A.; Bolch, T.; Stoffel, M.; Solomina, O.; Beniston, M. Climate change impacts on glaciers and runoff in Tien Shan (Central Asia). *Nat. Clim. Chang.* **2012**, *2*, 725–731. [CrossRef]
3. Viviroli, D.; Dürr, H.H.; Messerli, B.; Meybeck, M.; Weingartner, R. Mountains of the world, water towers for humanity: Typology, mapping, and global significance. *Water Resour. Res.* **2007**, *43*, 1–13. [CrossRef]
4. Farinotti, D.; Longuevergne, L.; Moholdt, G.; Duethmann, D.; Mölg, T.; Bolch, T.; Vorogushyn, S.; Güntner, A. Substantial glacier mass loss in the Tien Shan over the past 50 years. *Nat. Geosci.* **2015**, *8*, 716–722. [CrossRef]
5. Aizen, V.B.; Aizen, E.M.; Kuzmichonok, V.A. Glaciers and hydrological changes in the Tien Shan: Simulation and prediction. *Environ. Res. Lett.* **2007**, *2*, 045019. [CrossRef]
6. Aizen, V.B.; Kuzmichenok, V.A.; Surazakov, A.B.; Aizen, E.M. Glacier changes in the Tien Shan as determined from topographic and remotely sensed data. *Glob. Planet. Chang.* **2007**, *56*, 328–340. [CrossRef]
7. Hagg, W.; Braun, L.N.; Weber, M.; Becht, M. Runoff modelling in glacierized Central Asian catchments for present-day and future climate. *Nord. Hydrol.* **2006**, *37*, 93–105. [CrossRef]
8. Karthe, D.; Chalov, S.; Borchardt, D. Water resources and their management in central Asia in the early twenty first century: Status, challenges and future prospects. *Environ. Earth Sci.* **2015**, *73*, 487–499. [CrossRef]
9. Kaser, G.; Großhauser, M.; Marzeion, B. Contribution potential of glaciers to water availability in different climate regimes. *Natl. Acad. Sci. USA* **2010**, *107*, 20223–20227. [CrossRef]
10. Narama, C.; Kääb, A.; Duishonakunov, M.; Abdrakhmatov, K. Spatial variability of recent glacier area changes in the Tien Shan Mountains, Central Asia, using Corona (~1970), Landsat (~2000), and ALOS (~2007) satellite data. *Glob. Planet. Chang.* **2010**, *71*, 42–54. [CrossRef]
11. Vilesov, E.; Severskiy, I. Degradation of the Dzhungar (Zhetysu) Alatau Glaciation in the Second Half of the XX Century. *Ice Snow* **2013**, *53*, 12–20.
12. Severskiy, I.; Vilesov, E.; Kokarev, A.; Shesterova, I.; Morozova, V.; Kogutenko, L.; Usmanova, Z. Glacial systems of the Balkash-Alakol basin: State, modern changes. *Quest. Geogr. Geoecology* **2012**, *2*, 31–40.
13. Kaldybayev, A.; Chen, Y.; Vilesov, E. Glacier change in the Karatal river basin, Zhetysu (Dzhungar) Alatau, Kazakhstan. *Ann. Glaciol.* **2016**, *57*, 11–19. [CrossRef]
14. Kaldybayev, A.; Chen, Y.; Issanova, G.; Wang, H.; Mahmudova, L. Runoff response to the glacier shrinkage in the Karatal river basin, Kazakhstan. *Arab. J. Geosci.* **2016**, *9*, 208. [CrossRef]
15. Severskiy, I.; Vilesov, E.; Armstrong, R.; Kokarev, A.; Kogutenko, L.; Usmanova, Z.; Morozova, V.; Raup, B. Changes in glaciation of the Balkhash-Alakol basin, central Asia, over recent decades. *Ann. Glaciol.* **2016**, *57*, 382–394. [CrossRef]
16. Cherkasov, P. *Glacier Inventory of the USSR. Lake Balkhash Basin, Part 4*; Hydrometeorological Publishing House: Leningrad, Russia, 1975; Volume 13.
17. Cherkasov, P. *Glacier Inventory of the USSR. Lake Balkhash Basin, Part 5*; Hydrometeorological Publishing House: Leningrad, Russia, 1980; Volume 13.
18. Cherkasov, P. *Glacier Inventory of the USSR. Lake Balkhash Basin, Part 6*; Hydrometeorological Publishing House: Leningrad, Russia, 1970; Volume 13.
19. Cherkasov, P.; Erasov, V. *Glacier Inventory of the USSR. Lake Balkhash Basin, Part 7*; Hydrometeorological Publishing House: Leningrad, Russia, 1969; Volume 13.
20. Chen, Y.; Li, W.; Deng, H.; Fang, G.; Li, Z. Changes in Central Asia's Water Tower: Past, Present and Future. *Sci. Rep.* **2016**, *6*, 35458. [CrossRef] [PubMed]

21. Pritchard, H.D. Asia's shrinking glaciers protect large populations from drought stress. *Nature* **2019**, *569*, 649–654. [CrossRef]
22. Sorg, A.; Huss, M.; Rohrer, M.; Stoffel, M. The days of plenty might soon be over in glacierized Central Asian catchments. *Environ. Res. Lett.* **2014**, *9*, 104018. [CrossRef]
23. Vilesov, E.; Morozova, V.; Seversky, I. *Glaciation of the Dzungarian (Zhetysu) Alatau: Past, Present, Future*; KazNU: Almaty, Kazakhstan, 2013.
24. Yudichev, M. *Dzungarian Alatau. Materials on Geology and Minerals of Kazakhstan*; KazFAN USSR: Leningrad, Russia, 1940; Volume 14.
25. Ministry of Energy of the Republic of Kazakhstan United Nations Development Programme in Kazakhstan Global Environment Facility. *Seventh National Communication and Third Biennial Report of the Republic of Kazakhstan to the UN Framework Convention on Climate Change*; Ministry of Energy of the Republic of Kazakhstan United Nations Development Programme in Kazakhstan Global Environment Facility: Astana, Kazakhstan, 2017; p. 290.
26. Ministry of Ecology, Geology and Natural Resources of the Republic of Kazakhstan; Republican State Enterprise «Kazhydromet»; Scientific Research Center. *Annual Bulletin of Monitoring of the Climate State and Climate Change in Kazakhstan: 2021*; Research Center of RSE "Kazhydromet": Astana, Kazakhstan, 2022; p. 76.
27. Cherednichenko, A.; Cherednichenko, A.; Vilesov, E.N.; Cherednichenko, V.S. Climate change in the City of àlmaty during the past 120 years. *Quat. Int.* **2015**, *358*, 101–105. [CrossRef]
28. Hollander, M.; Wolfe, D.A. *Nonparametric Statistical Methods*; John Wiley & Sons.: Hoboken, NJ, USA, 1999.
29. Paul, F.; Barrand, N.E.; Baumann, S.; Berthier, E.; Bolch, T.; Casey, K.; Frey, H.; Joshi, S.P.; Konovalov, V.; Le Bris, R.; et al. On the accuracy of glacier outlines derived from remote-sensing data. *Ann. Glaciol.* **2013**, *54*, 171–182. [CrossRef]
30. Racoviteanu, A.E.; Paul, F.; Raup, B.; Khalsa, S.J.S.; Armstrong, R. Challenges and recommendations in mapping of glacier parameters from space: Results of the 2008 global land ice measurements from space (GLIMS) workshop, Boulder, Colorado, USA. *Ann. Glaciol.* **2009**, *50*, 53–69. [CrossRef]
31. Paul, F.; Kääb, A. Perspectives on the production of a glacier inventory from multispectral satellite data in Arctic Canada: Cumberland Peninsula, Baffin Island. *Ann. Glaciol.* **2005**, *42*, 59–66. [CrossRef]
32. Bolch, T. Climate change and glacier retreat in northern Tien Shan (Kazakhstan/Kyrgyzstan) using remote sensing data. *Glob. Planet. Chang.* **2007**, *56*, 1–12. [CrossRef]
33. Bolch, T.; Yao, T.; Kang, S.; Buchroithner, M.F.; Scherer, D.; Maussion, F.; Huintjes, E.; Schneider, C. A glacier inventory for the western Nyainqentanglha range and the Nam Co Basin, Tibet, and glacier changes 1976–2009. *Cryosphere* **2010**, *4*, 419–433. [CrossRef]
34. Paul, F.; Bolch, T.; Briggs, K.; Kääb, A.; McMillan, M.; McNabb, R.; Nagler, T.; Nuth, C.; Rastner, P.; Strozzi, T.; et al. Error sources and guidelines for quality assessment of glacier area, elevation change, and velocity products derived from satellite data in the Glaciers_cci project. *Remote Sens. Environ.* **2017**, *203*, 256–275. [CrossRef]
35. Farooq, I.; Shah, A.R.; Salik, K.M.; Ismail, M. Annual, Seasonal and Monthly Trend Analysis of Temperature in Kazakhstan During 1970–2017 Using Non-parametric Statistical Methods and GIS Technologies. *Earth Syst. Environ.* **2021**, *5*, 575–595. [CrossRef]
36. Talipova, E.; Shrestha, S.; Alimkulov, S.; Nyssanbayeva, A.; Tursunova, A.; Isakan, G. Influence of climate change and anthropogenic factors on the Ile River basin streamflow, Kazakhstan. *Arab. J. Geosci.* **2021**, *14*, 1756. [CrossRef]
37. Shahgedanova, M.; Afzal, M.; Severskiy, I.; Usmanova, Z.; Saidaliyeva, Z.; Kapitsa, V.; Kasatkin, N.; Dolgikh, S. Changes in the mountain river discharge in the northern Tien Shan since the mid-20th Century: Results from the analysis of a homogeneous daily streamflow data set from seven catchments. *J. Hydrol.* **2018**, *564*, 1133–1152. [CrossRef]
38. Kriegel, D.; Mayer, C.; Hagg, W.; Vorogushyn, S.; Duethmann, D.; Gafurov, A.; Farinotti, D. Changes in glacierisation, climate and runoff in the second half of the 20th century in the Naryn basin, Central Asia. *Glob. Planet. Chang.* **2013**, *110*, 51–61. [CrossRef]
39. Zhang, Q.; Chen, Y.; Li, Z.; Li, Y.; Xiang, Y.; Bian, W. Glacier changes from 1975 to 2016 in the Aksu River Basin, Central Tianshan Mountains. *J. Geogr. Sci.* **2019**, *29*, 984–1000. [CrossRef]
40. Zhang, Q.; Chen, Y.; Li, Z.; Fang, G.; Xiang, Y.; Li, Y.; Ji, H. Recent changes in water discharge in snow and glacier melt-dominated rivers in the tienshan mountains, Central Asia. *Remote Sens.* **2020**, *12*, 2704. [CrossRef]
41. Kutuzov, S.; Shahgedanova, M. Glacier retreat and climatic variability in the eastern Terskey-Alatoo, inner Tien Shan between the middle of the 19th century and beginning of the 21st century. *Glob. Planet. Chang.* **2009**, *69*, 59–70. [CrossRef]
42. He, Y.; Yang, T.-b.; Ji, Q.; Chen, J.; Zhao, G.; Shao, W.-W. Glacier variation in response to climate change in Chinese Tianshan Mountains from 1989 to 2012. *J. Mt. Sci.* **2015**, *12*, 1189–1202. [CrossRef]
43. Aizen, V.B.; Kuzmichenok, V.A.; Surazakov, A.B.; Aizen, E.M. Glacier changes in the central and northern Tien Shan during the last 140 years based on surface and remote-sensing data. *Ann. Glaciol.* **2006**, *43*, 202–213. [CrossRef]
44. Narama, C.; Shimamura, Y.; Nakayama, D.; Abdrakhmatov, K. Recent changes of glacier coverage in the western Terskey-Alatoo range, Kyrgyz Republic, using Corona and Landsat. *Ann. Glaciol.* **2006**, *43*, 223–229. [CrossRef]
45. Unger-Shayesteh, K.; Vorogushyn, S.; Farinotti, D.; Gafurov, A.; Duethmann, D.; Mandychev, A.; Merz, B. What do we know about past changes in the water cycle of Central Asian headwaters? A review. *Glob. Planet. Chang.* **2013**, *110*, 4–25. [CrossRef]
46. Tielidze, L.G.; Wheate, R.D. The Greater Caucasus Glacier Inventory (Russia, Georgia and Azerbaijan). *Cryosphere* **2018**, *12*, 81–94. [CrossRef]
47. Tennant, C.; Menounos, B.; Wheate, R.; Clague, J.J. Area change of glaciers in the Canadian rocky mountains, 1919 to 2006. *Cryosphere* **2012**, *6*, 1541–1552. [CrossRef]

48. Paul, F.; Rastner, P.; Azzoni, R.S.; Diolaiuti, G.; Fugazza, D.; Bris, R.L.; Nemec, J.; Rabatel, A.; Ramusovic, M.; Schwaizer, G.; et al. Glacier shrinkage in the Alps continues unabated as revealed by a new glacier inventory from Sentinel-2. *Earth Syst. Sci. Data* **2020**, *12*, 1805–1821. [CrossRef]
49. Kokarev, A.; Shesterova, I. Present-day changes of mountain glaciers on the southern slope of the Dzhungarian Alatau range. *Ice Snow* **2015**, *128*, 54. [CrossRef]
50. Dolgushin, L.; Osipova, G. The Nature of the World: Glaciers. Mysl. Moscow, USSR. 1989; Volume 447. Available online: https://www.studmed.ru/dolgushin-l-d-osipova-g-b-ledniki_e961d16f14e.html (accessed on 1 March 2023).
51. Liu Chaohai; Han Tianding Relation between recent glacier variations and climate in the Tien Shan Mountains, Central Asia. *Ann. Glaciol.* **1992**, *16*, 11–16. [CrossRef]
52. Pieczonka, T.; Bolch, T. Region-wide glacier mass budgets and area changes for the Central Tien Shan between ~1975 and 1999 using Hexagon KH-9 imagery. *Glob. Planet. Chang.* **2015**, *128*, 1–13. [CrossRef]
53. Li, B.; Zhu, A.X.; Zhang, Y.; Pei, T.; Qin, C.; Zhou, C. Glacier change over the past four decades in the middle Chinese Tien Shan. *J. Glaciol.* **2006**, *52*, 425–432. [CrossRef]
54. Aizen, V.B.; Aizen, E.M.; Melack, J.M.; Dozier, J. Climatic and hydrologic changes in the Tien Shan, central Asia. *J. Clim.* **1997**, *10*, 1393–1404. [CrossRef]
55. Qin, D.; Liu, S.; Li, P. Snow cover distribution, variability, and response to climate change in western China. *J. Clim.* **2006**, *19*, 1820–1833. [CrossRef]
56. Bahr, D.B.; Pfeffer, W.T.; Sassolas, C.; Meier, M.F. Response time of glaciers as a function of size and mass balance: 1. Theory. *J. Geophys. Res. Solid Earth* **1998**, *103*, 9777–9782. [CrossRef]
57. Ye, B.; Ding, Y.; Liu, C. Response of valley glaciers in various sizes and their runoff to climate change. *J. Glaciol.* **2003**, *49*, 1–7.
58. Granshaw, F.D.; Fountain, A.G. Glacier change (1958–1998) in the North Cascades National Park Complex, Washington, USA. *J. Glaciol.* **2006**, *52*, 251–256. [CrossRef]
59. Ciais, P.; Sabine, C.; Bala, G.; Bopp, L.; Brovkin, V.; Canadell, J.; Chhabra, A.; DeFries, R.; Galloway, J.; Heimann, M.; et al. The physical science basis. Contribution of working group I to the fifth assessment report of the intergovernmental panel on climate change. *Chang. IPCC Clim.* **2013**, *375*, 20160321. [CrossRef]
60. Vandenberghe, J.; Renssen, H.; van Huissteden, K.; Nugteren, G.; Konert, M.; Lu, H.; Dodonov, A.; Buylaert, J.P. Penetration of Atlantic westerly winds into Central and East Asia. *Quat. Sci. Rev.* **2006**, *25*, 2380–2389. [CrossRef]
61. Hagg, W.; Mayer, C.; Lambrecht, A.; Kriegel, D.; Azizov, E. Glacier changes in the Big Naryn basin, Central Tian Shan. *Glob. Planet. Chang.* **2013**, *110*, 40–50. [CrossRef]
62. Gulnura, I.; Abuduwaili, J.; Oleg, S. Deflation processes and their role in desertification of the southern Pre-Balkhash deserts. *Arab. J. Geosci.* **2014**, *7*, 4513–4521. [CrossRef]
63. Wang, L.; Li, Z.; Wang, F.; Edwards, R. Glacier shrinkage in the Ebinur lake basin, Tien Shan, China, during the past 40 years. *J. Glaciol.* **2014**, *60*, 245–254. [CrossRef]
64. Ageta, Y.; Kadota, T. Predictions of changes of glacier mass balance in the Nepal Himalaya and Tibetan Plateau: A case study of air temperature increase for three glaciers. *Ann. Glaciol.* **1992**, *16*, 89–94. [CrossRef]
65. Fujita, K.; Ageta, Y. Effect of summer accumulation on glacier mass balance on the Tibetan Plateau revealed by mass-balance model. *J. Glaciol.* **2000**, *46*, 244–252. [CrossRef]